



Toxicological effects of long-term continuous exposure to ambient air on human bronchial epithelial Calu-3 cells exposed at the air-liquid interface

E.J. Zimmermann^{a,b}, A. Das^{a,b}, A. Huber^{a,b}, N. Gawlitta^a, E. Kuhn^a, C. Schlager^c, B. Gutmann^c, T. Krebs^c, J. Schnelle-Kreis^a, M.N. Delaval^{a,*}, R. Zimmermann^{a,b}

^a Joint Mass Spectrometry Center (JMSC) at Comprehensive Molecular Analytics (CMA), Helmholtz Zentrum München, Munich, 85764, Germany

^b Joint Mass Spectrometry Center (JMSC) at Analytical Chemistry, Institute of Chemistry, University of Rostock, Rostock, 18051, Germany

^c Vitrocell Systems GmbH, 79183, Waldkirch, Germany

ARTICLE INFO

Keywords:

Ambient air toxicity
Air-liquid interface lung cell model
Automated exposure system
Polycyclic aromatic hydrocarbons
Aerosol continuous exposure
Physicochemical aerosol characterization

ABSTRACT

Air pollution significantly contributes to the global burden of respiratory and cardiovascular diseases. While single source/compound studies dominate current research, long-term, multi-pollutant studies are crucial to understanding the health impacts of environmental aerosols. Our study aimed to use the first air-liquid interface (ALI) aerosol exposure system adapted for long-term *in vitro* exposures for ambient air *in vitro* exposure.

The automated exposure system was adapted to enable long-term cell exposure. ALI human bronchial epithelial cells (Calu-3) were continuously exposed for 72 h to the ambient air from a European urban area (3 independent exposures). Experimental evaluation included comprehensive toxicological assessments coupled to physical and chemical characterization of the aerosol. Exposure to ambient air resulted in increased significant cytotoxicity and a non-significant decrease in cell viability. Differential gene expressions were indicated for genes related to inflammation (*IL1B*, *IL6*) and to xenobiotic metabolism (*CYP1A1*, *CYP1B1*) with possible correlations to the PM_{2.5} content. Common air pollutants were identified such as the carcinogenic benz[a]pyrene (≤ 3.4 ng m⁻³/24h) and PM_{2.5} (≤ 11.6 µg m⁻³/24h) with a maximum particle number mean of 4.4×10^{-3} m³/24h.

For the first time, ALI human lung epithelial cells were exposed for 72 h to continuous airflow of ambient air. Despite direct exposure to ambient aerosols, only small decrease in cell viability and gene expression changes was observed. We propose this experimental set-up combining comprehensive aerosol characterization and long-term continuous ALI cell exposure for the identification of hazardous compounds or compound mixtures in ambient air.

1. Introduction

Air pollution is one of the major public health concerns causing significant economic, environmental, and human health impacts. Each year, millions of premature deaths are estimated to be caused by air pollution (EEA, 2021; WHO, 2021a). Ambient air pollution increased especially in industrial and urban regions in the last 20 years, making it now one of the major risk factors on the global burden of diseases (Murray et al., 2020). Aerosols polluting ambient air are complex mixtures of compounds that can be largely categorized as gases, (semi-) volatile organic compounds (SVOCs) and particulate matter (PM), consisting of organic and inorganic compounds. Despite the many different sources of air pollutants, a major proportion are produced by vehicle exhausts and are thus higher concentrated in urban compared to rural

areas (Reinmuth-Selzle et al., 2017).

Adverse health effects have been linked to all categories of ambient air pollution but exposure to PM is the most studied category causing strong adverse effects on human health (Brook et al., 2010; Kelly and Fussell, 2012; Wei et al., 2023). It has been demonstrated that ambient PM increases all-cause mortality and has negative impacts on respiratory, cardiometabolic health, cognitive health, and childhood development (Aguilera et al., 2016; Kyung and Jeong, 2020; Thurston and Rice, 2019). The adverse effects, location and mode of action of PM vary according to their size, as they can reach and deposit in various regions of the respiratory tract or act as carriers for other compounds (Ohlwein et al., 2019; Kwon et al., 2020). The effect of polluted ambient air was demonstrated by many epidemiological studies (Brunekreef et al., 2009; Kim et al., 2021; Ranzani et al., 2023; Tsai et al., 2019) and *in vivo/ex*

* Corresponding author.

E-mail address: mathilde.delaval@helmholtz-munich.de (M.N. Delaval).

<https://doi.org/10.1016/j.envres.2025.120759>

Received 11 September 2024; Received in revised form 18 December 2024; Accepted 2 January 2025

Available online 2 January 2025

0013-9351/© 2025 The Authors. Published by Elsevier Inc. This is an open access article under the CC BY-NC license (<http://creativecommons.org/licenses/by-nc/4.0/>).

vivo studies (Ghio, 1999; Kurtz et al., 2024; Morgan et al., 2011; Strak et al., 2013). However, studies indicating the involved cellular mechanisms or the combined toxicity of compounds present in polluted ambient air are still scarce (Forest, 2021). This is primarily due to the complex mixture of compounds in ambient air and the lack of efficient exposure system coupled to reproducible *in vitro* models. Lu et al. (2017) showed that, while exposure to silica nanoparticles or lead alone did not trigger apoptosis in human alveolar epithelial A459 cells, co-exposures to silica nanoparticles and lead caused a synergistic effect with increased apoptotic changes. In previous studies, we also demonstrated that subsequent *in vitro* exposures to allergens and air pollutants altered the cellular and molecular responses of bronchial epithelial cells (Candeias et al., 2022; Zimmermann et al., 2023). Moreover, it has been suggested that, even when the toxicity of single compounds is well characterized, mixture of these compounds could induce unexpected effects, including increased oxidative stress, inflammation or DNA damage (Jiang et al., 2020; Zheng et al., 2012). Taken together, these findings indicate a significant knowledge gap and highlight the need to evaluate pollutant combinations for better representing real-life conditions (Forest, 2021).

For addressing this knowledge gap, fast and low cost mechanistical *in vitro* studies with ambient air at different locations can be used but are technically challenging. Performing such realistic *in vitro* ambient air exposures at the air liquid interface (ALI) requires long-term exposure to assess the effects of low dose air pollutants and thus, a suitable aerosol cell exposure system. This system needs to provide stable and controlled conditions while performing extended exposure durations. Factors such as precise temperature, humidity control, homogenous airflow and particle distribution are vital considerations in the development of such a system. Currently, there are mainly two ALI exposure techniques in use, single short exposures with e.g. a nebulization unit (Bredeck et al., 2023) and continuous airflow exposures (Lucci et al., 2018; Mühlhopt et al., 2016). Short single exposures have the advantage of using defined single dose of pollutants for testing their acute toxicological effects, but for testing long-term effects of pollutants at low doses, a continuous airflow exposure system is needed, enabling more realistic exposure conditions.

Robust *in vitro* cell model systems, representative of the human airways, are also required for evaluating the effects of long-term exposures to air pollutants. Various *in vitro* cell culture models are already established at ALI for mimicking pulmonary exposure, such as alveolar or bronchial epithelial cell lines, A549 cells, BEAS-2B cells or 16HBE14o-cells (Rothen-Rutishauser et al., 2023; Upadhyay and Palmberg, 2018). However, most of these models are not suitable for assessing the potential toxicity of airborne particles and gaseous compounds following long-term exposures because they remain viable for only a few days when cultured at the ALI or start to overgrow (Braakhuis et al., 2020; He et al., 2021). For our study, the use of the human bronchial epithelial Calu-3 cell line was the most suitable for long-term exposures, because Calu-3 cells form a monolayer epithelium and tight junctions. Once differentiated, they can be cultured for weeks at the ALI and withstand the airflow of continuous exposure systems. In the present study, we aimed 1) to test the first automated exposure system (AES) that allows long-term exposures of *in vitro* cell cultures at the air liquid interface (ALI) to a continuous flow of aerosol, and 2) to investigate the toxicological effects of ambient air pollution on bronchial epithelial Calu-3 cells cultured and exposed at the air-liquid interface to a continuous airflow of ambient air for 72 h. We aimed to improve our understanding of the cellular responses caused by long-term exposures to ambient air pollution, their underlying cellular mechanisms and contribute to the advancement of the exposure system for studying ambient air exposure.

2. Method

2.1. Cells and cell culturing

Human bronchial epithelium Calu-3 cell line were purchased from Elabscience (China American Tissue Culture Collection (ATCC, Rockville, USA). Calu-3 cells were cultured according to Braakhuis et al. (2020) in minimal essential medium (MEM) containing GlutaMAX, supplemented with 10% fetal bovine serum (FBS), 1% non-essential amino acid (NEAA) solution and 1% penicillin/streptomycin (P/S) in an incubator with 5% CO₂ at 37 °C. Upon reaching about 80% confluence, Calu-3 cells were detached from the culture flask with 0.05% trypsin-EDTA. Cell suspension (1 mL) with a density of 5×10^5 cells mL⁻¹ was seeded into the apical side of a sterile 24 mm Costar insert (0.4 µm pore size, 4.67 cm² polyester membrane) placed in a 6-well plate. 1.5 mL culture medium was added to the basolateral side of the insert for nutrient supply. After 7 days under submerged conditions, a confluent cell layer was obtained, the apical medium was removed, and the cells were washed once with Hank's Balanced Salt Solution (HBSS). Calu-3 cells were further cultured at ALI for 7 days and the basolateral medium was refreshed every 2–3 days. Cell culture medium and supplements were purchased from Life Technologies (Thermo Fisher Scientific Inc., The Netherlands).

2.2. Adaptation of an automated exposure station (AES) for long-term exposures

A custom-made VITROCELL® automated exposure station extended version (AES, Vitrocell Systems GmbH), previously described in (Mühlhopt et al., 2016), was used and adapted for long-term exposures. Fig. 1 shows the system with the additional and improved parts (in orange) enabling long-term cell exposures to continuous air flow and Table 1 indicates the additional and improved parts in detail.

To maintain the temperature and humidity stability of the aerosols, a heated inlet, relocated humidification units, additional heaters/fans and an additional water circulation bath were installed. Together with additional sensors for relative humidity and temperature inside the exposure modules for clean air and aerosol, a cloud-based application was programmed and implemented allowing the recording of respective values at cellular level and online adjustment of those parameters. Additionally, all instrument settings and sensor readouts were automatically logged, to observe potential variability between exposures. To further reduce the onsite maintenance and protect the humidity sensitive parts of the system, a water re-fill system was installed, for re-filling the water tanks of the humidification units, as well as an additional cooled water trap directly before the main mass flow controller.

2.3. In-vitro cell exposures

Directly before exposure, cells were placed inside the exposure modules, containing 6.5 mL of exposure medium (MEM-GlutaMAX, 2.5% FBS, 1% NEAA, 1% P/S and 25 mM HEPES-EDTA) per bucket. Cells were constantly exposed for 72h to clean air (CA) or ambient air (AA) from an urban area in southern Munich, Germany. The aerosol was sampled from the outside of the lab with a 10 m sampling line, conducted to the online instruments for aerosol characterization and sampling, and further guided to the AES. The aerosol was first guided through the heated inlet (set to 37 °C) and then through a size-selective impactor for exclusion of particles with size fractions bigger than 2.5 µm. The aerosol was further guided to the AES reactor and conditioned to 37 °C ± 0.2 °C and 86.5% ± 1.5% rH before reaching the cells via the isokinetic sampling for each position of the exposure modules. Total aerosol flow into the AES was 16.6 L min⁻¹ and the flow over the cells was 50 mL min⁻¹ for each insert. The cabinet temperature was set to 37.8 °C and the module temperature was cooled down with the external water circulation bath to 37 °C ± 0.1 °C. Six inserts with cells placed for

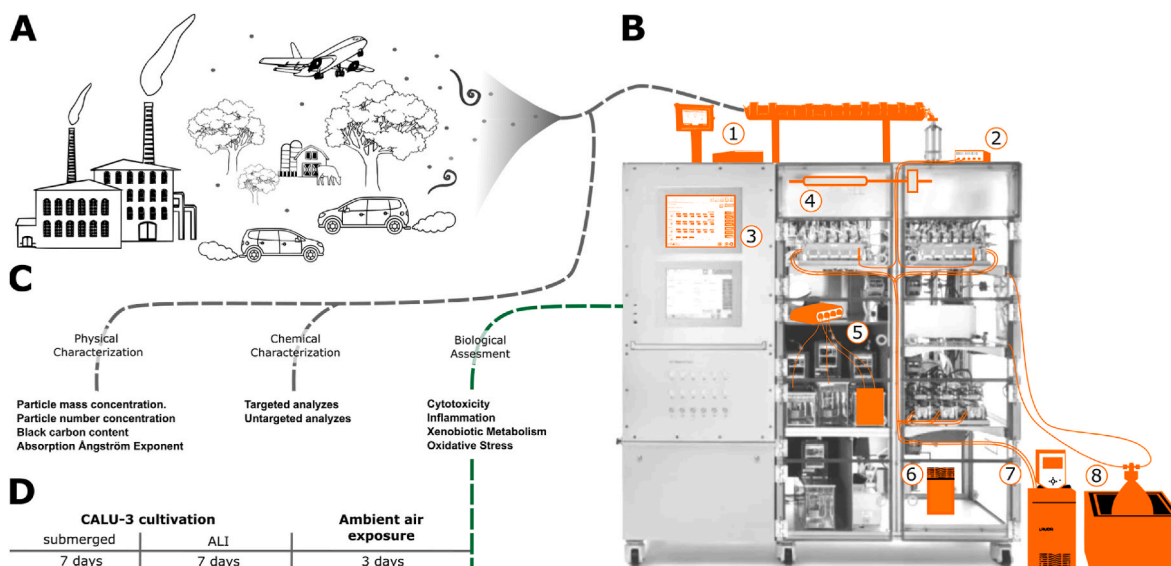


Fig. 1. Experimental overview of long-term exposure and the adaptations of the system illustrated. (A) Ambient aerosol. (B) Adapted advanced automated exposure system (AES), the adapted parts are highlighted in orange. Further details are given in Table 1. (C) Aerosol characterization, and biological assessments performed. (D) Timeline of Calu-3 cell line cultivation and exposure. (For interpretation of the references to colour in this figure legend, the reader is referred to the Web version of this article.)

Table 1
Additional and improved AES parts for continues long-term exposure.

| Parts | Description |
|-------------------------------|--|
| 1 Heated inlet | Installation of a heated inlet (37 °C) for enhancing the stability of the aerosol temperature and humidity. |
| 2 Module sensors | Deployment of a set of sensors placed inside the exposure (ambient air (AA) and clean air (CA)) modules for measuring constantly the relative humidity (rH) and temperature (T) at the cellular level. |
| 3 Settings/Remote Control | Installation of a cloud-based application programmed for observing and regulating relevant parameters of the system remotely. |
| 4 Humidification Unit | Relocation of the humidification unit allowing a more stable humidification of rH 86.5% ± 1.5%. |
| 5 Water re-fill system | Installation of an automated water re-fill system for both circulation baths (connected to the humidification units) for increasing their autonomy time. |
| 6 Additional Heaters and Fans | Placement of 4 additional heaters and 4 additional ventilation fans in the system allowing homogenous temperature distribution throughout the system. |
| 7 Water circulation bath | Installation of an additional water circulation bath with cooling function outside of the system, allowing precise and stable temperature at the cellular stage of 37 °C ± 0.2 °C. |
| 8 Cooled water trap | Addition of a cooled water-trap before the humidity sensitive controllers for reduction of humidity in the exhaust aerosol. |

72 h in an incubator (37 °C, without CO₂) with the same volume of exposure media served as incubator controls (Inc).

2.4. Aerosol characterization

2.4.1. Online aerosol measurements

Online characterization of the aerosol was done in parallel to the AES exposures and focused especially on PM_{2.5}, considering that long-term exposures to low doses of PM_{2.5} were shown to cause chronic adverse health effects (Cho et al., 2018; Hsiao et al., 2000; Weber et al., 2016). A Condensation Particle Counter (CPC model 3750, TSI, USA) and a Tapered Element Oscillating Microbalance (TEOM 1400a, Thermo Fisher Scientific) measured the particle number concentration and mass

concentration, respectively. An Aethalometer (AE33, Magee Scientific) was installed to measure the equivalent Black Carbon (eBC) and the Absorption Ångström Exponent (AAE). eBC refers to the black carbon concentration indirectly derived by optical measurements of attenuation of light by aerosol (Petzold et al., 2013). The eBC is measured at the wavelength of 880 nm using its corresponding mass absorption cross-section (MAC) value of 7.77 m²/g (Drinovec et al., 2015). The absorption Ångström exponent (AAE) characterizes how the absorption of light by aerosols changes across different wavelengths in the spectrum. The wavelength pair of 470 nm and 950 nm were used in this study as suggested by Zotter et al. (2017) for ambient aerosol. The MAC values used were 14.54 m²/g and 7.19 m²/g for 470 nm and 950 nm respectively (Drinovec et al., 2015). Values given in the text are the median ±95 % confidence interval.

2.4.2. Offline aerosol measurements

Sampling of the particulate phase aerosol was done on Quartz fiber filters (QFF, Whatman Cytiva) parallel to online aerosol instruments and the ALI. These filters were pre-heated at 550 °C for 5 h prior to use. The filter samples were taken every 24 h of the 72-h period to minimize the volatilization losses. The sampling period for each sample was 24 h at a flowrate of 0.6 m³h⁻¹. After sampling, the filters were stored at -25 °C till further analysis. Respective field blanks were collected where the filters were put inside the sampler without any flows.

Non-targeted determination of the PM samples was conducted using direct thermal desorption comprehensive two-dimensional gas chromatography time-of-flight mass spectrometry (DTD-GC × GC-TOFMS, Pegasus BT4D, Leco) according to Gawlitta et al. (2023). An Optic-4 inlet system (GL Sciences) was utilized. For the DTD method, a filter punch of 3 mm for each 24 h sample was used and the three filter punch samples, corresponding to the respective 72 h exposure were combined in one glass liner for analysis. The 72-h sample corresponded to 0.72 m³ sampled air. 1 µL of deuterated standard (ISTD) was applied to the filter sample prior analysis. A non-polar (BPX5)/polar (BPX50) column setup was installed for the GC × GC separation. A pre-column (BPX5) was additionally installed. GC temperature was initially held at 50 °C for 5 min, increased to 150 °C at a rate of 5 °C min⁻¹ and from 150 °C at a rate of 3 °C min⁻¹ up to 340 °C. The final temperature was held for 15 min. Transfer line and ion source temperature were set to 300 °C and 250 °C, respectively. Mass acquisition was performed in the range of 29–600 Da

at an acquisition rate of 100 spectra/s. The electron energy applied was 70 eV. Data acquisition and processing was performed using the ChromaTOF software (Version 5.5, Leco). Peak finding was conducted at a signal-to-noise (S/N) of 100. The classification was realized using retention time and mass spectral filters. More information on the thermal desorption, chromatographic and classification methods can be found in the Supplementary Material (Tables S1–S5).

Quantification of targeted PAHs was done with a Gas Chromatograph Mass Spectrometer (Shimadzu GCMS-QP2010 Ultra, Shimadzu) according to Das et al. (2024). PAHs were used for in-depth analysis due to increasing evidence, linking them to a variety of different chronic diseases, including respiratory diseases and their involvement in various immune system dysregulation (Ravanbakhsh et al., 2023; Yu et al., 2022). The QFF samples were cut using defined punches ($d = 10$ mm) each representing 0.9 m^3 of the sampled air, spiked with deuterated PAHs standards ($1 \mu\text{L}$ of an internal standard (ISTD)) and then transferred into glass liners to be analyzed using the direct thermal desorption unit (Schnelle-Kreis et al., 2005; Orasche et al., 2011). The measurements for each sample were conducted at least twice to ensure the reproducibility of the results.

2.5. Epithelial integrity, cytotoxicity, and cell viability evaluation

After exposure, the epithelial cell layer integrity was examined by transepithelial electrical resistance (TEER) measurement. Briefly, the inserts were placed into clean 6-well plates (Costar), and 1.0 and 1.5 mL of pre-warmed Hanks's Balanced Salt Solution (HBSS) were added to the apical and basolateral Transwell® chambers, respectively. The TEER value of each cellular monolayer was measured using a volt-ohmmeter (EVOM3), equipped with STX3 chopstick electrodes (World Precision Instruments).

Epithelial integrity after exposure was also evaluated with Life/Dead cell staining. Cells were washed twice with pre-warmed HBSS and then incubated for 30 min at 37°C with freshly prepared staining solution [Hoechst 33342 nucleic acid stain, $5 \mu\text{g mL}^{-1}$ (Sigma-Aldrich; B2261) and propidium iodide (PI), $25 \mu\text{g mL}^{-1}$ (Sigma-Aldrich; P41770) prepared in HBSS]. Following staining, cells were then washed again twice with pre-warmed HBSS and HBSS was added in both insert compartments before analysis. Hoechst (Ex: 350 nm, Em: 461 nm) and PI (Ex: 535 nm, Em: 617 nm) fluorescence was recorded with a live cell microscope (LionheartFX automated microscope, Agilent).

Cell viability was determined directly after exposure by measuring the metabolic activity of the cells by the resazurin assay (CellTiter-Blue® Cell Viability Assay, Promega) (Hamid et al., 2004). This assay is based on the reduction of the blue non-fluorescent dye resazurin to the pink, fluorescent resorufin by mitochondrial and cytosolic enzymes. Briefly, cells were washed once with warmed HBSS and then incubated for 45 min at 37°C , in the dark with resazurin diluted in complete cell culture medium. Afterwards, the reduction of resazurin in resorufin, emitting fluorescence at 590 nm, was recorded with a spectrophotometer (MULTISKAN SKY Microplate Spectrophotometer, ThermoFisher Scientific) plate reader. The results are presented in percentage compared to Incubator control, representing 100% of metabolic activity.

Cell death was evaluated by measuring the release of the cytosolic Lactate dehydrogenase (LDH), indicating the rupture of the cell membranes, a marker of cell death by necrosis (Decker and Lohmann-Matthes, 1988). The LDH release assay (Cytotoxicity Detection Kit, Roche) was performed according to the manufacturer's instructions. The basolateral medium as well as the apical cell wash with Hanks' Balanced Salt Solution (HBSS, Gibco) were collected for the determination of the extracellular LDH release. As positive controls, incubator control cells were lysed with 2% Triton X-100 (Sigma-Aldrich) for 20 min before harvest to determine the maximum LDH release. The results are presented as percentages compared to the positive control (Triton X-100) indicating 100% cytotoxicity.

Tight junctions were stained with the monoclonal antibody ZO-1

(Thermo Fisher Scientific; MA339100A647). Briefly, cells were washed once with PBS to remove apical secretions and fixed with 4% paraformaldehyde for 30 min at RT. Membranes were cut out and after washing with PBS (0.1% BSA), cells were permeabilized with 0.25% Triton X-100 for 15 min at room temperature, washed 3 times with PBS (0.1% BSA) and then blocked with 3% BSA in PBS (blocking solution) for 1 h. Cells were stained with a ZO-1 Monoclonal antibody, AlexaFluor 647 conjugate (Invitrogen, MA3339100A647) at a dilution of $2.5 \mu\text{g mL}^{-1}$ in blocking solution and DAPI ($1 \mu\text{g mL}^{-1}$) in the dark for 1 h. After washing 3 times with PBS, cells were embedded in Glycergel (DAKO, #C0563). Images were taken on a BioTek Microscope at 20x magnification.

2.6. Pro-inflammatory response and gene expression evaluation

For analyzing the release of the pro-inflammatory interleukins IL-6 and IL-8 in the collected sample media, DuoSet® ELISA Kits (ELISA, R&D Systems, DY206, DY208) were used. The assays were carried out according to the manufacturer's instructions. 3,3',5,5'-tetramethylbenzidine (TMB; Cell Signaling Technology, 7004P6) was used as chromogenic substrate and the absorbance was measured at 450 nm and 540 nm with the Varioskan™ Lux multimode microplate reader. Results in pg mL^{-1} are presented as mean \pm SD ($n \geq 3$ biological replicates, from individual exposures).

For evaluation of gene expression, cells were processed immediately after exposure, and stored in RNeasy Protect Cell Reagent (QIAGEN) for up to 1 month at -80°C . For RNA extraction, the RNeasy Plus Mini Kit (QIAGEN) was used with 1% β -mercaptoethanol (Roth) according to the manufacturer's protocol. Complementary DNA (cDNA) was synthesized from 250 ng total RNA using a high capacity cDNA Reverse Transcription Kit with RNase Inhibitor (Applied Biosystems) according to the manufacturer's instruction in a $20 \mu\text{L}$ reaction. Following cDNA synthesis, cDNA was diluted at $5 \text{ ng}/\mu\text{L}$ with nuclease-free water. Real-time PCR (RT-PCR) was performed in a total volume of $11 \mu\text{L}$ containing $2 \mu\text{L}$ cDNA, $3.5 \mu\text{L}$ nuclease-free water, $5 \mu\text{L}$ TaqMan Universal Master Mix and $0.5 \mu\text{L}$ TaqMan Gene Expression assay per reaction. QuantStudio3 cyclor (Applied Biosystems) was used for amplification. The gene expression of CXCL8, IL6, IL1 β , TLR2, HMOX1, CYP1A1, CYP1B1, CYP29) was normalized against two housekeeping genes (GAPDH, RFP13A) and expressed as \log_2 fold change compared with the incubator controls as calculated by the $\Delta\Delta\text{Ct}$ method (Livak and Schmittgen, 2001). Additional information on genes and their TaqMan assay used can be found in Table S6.

Malondialdehyde (MDA) release is an indicator of lipid peroxidation and can be used as a biomarker for cellular oxidative stress. Extracellular MDA was measured in the basolateral medium by using liquid-chromatography triple quadrupole mass spectrometry (LC-MS/MS) (API 4000 Triple Quadrupole system, AB Sciex in positive MRM mode) as previously described (Ren et al., 2017). Samples were first derivatized with 2,4-dinitrophenylhydrazine (DNPH) following subsequent extraction with liquid-liquid extraction before chromatographic separation on a C18 column (Agilent 1290 UHPLC System) in isocratic conditions. Data is presented as ng mL^{-1} MDA release in the basolateral medium and results are represented as mean \pm SD of three different positions in the system.

2.7. Statistical analysis and data processing

Statistical analysis and illustrations were performed in programming environment R (version 4.3.1) (Team, 2020) using the interface RStudio (Version, 2023.06.1, RStudio, Inc) (RStudio, 2020). Variability caused by the intrinsic state of the cells and not by the differential exposures were handled by normalizing to the CA control and focusing on the effect of AA exposed cells compared to CA exposed cells. Outliers were not identified. One position in the ambient air exposure modules was excluded, after identifying it as malfunctioning in subsequent

experiments. Sample size for our study was estimated according to Cohen (2013) and calculated in R with the pwrss package (Bulus, 2023) to be. Statistical power evaluation (parameter assumption: 3 group anova, effect size of 0.55–0.82 and sign. level 0.05) was done with the pwr package following effect size calculation (effectsize package: WE = 0.82, WW = 0.55, WWH = 0.81). In all cases, variance homogeneity was first tested with the Levene test between the different groups or samples. In case of similar variances and comparison of more than two groups, a two-way ANOVA (analysis of variance) was used followed by Tukey's honestly significant difference (HSD) test, to account for multiple testing. Pairwise comparison was performed with a two-tailed *t*-test to test for changes independent of the direction (increase or decrease). In case of inhomogeneous variances, a Welch's two-tailed *t*-test was applied. As there were no relevant and significant differences in all biological response from cells exposed with both used trumpet geometries, the samples were evaluated as biological replicates.

3. Results

3.1. Adaptations of the AES for long-term exposures

Prior to performing the long-term cell exposures, the adapted AES was validated, calibrated and critical factors were identified.

- Temperature and relative humidity (rH): Improving the stability of temperature and humidity in the system with independent read out in the exposure modules allowed for long-term cell exposures conditions ($37\text{ °C} \pm 0.1\text{ °C}$, $86.5\% \pm 1.5\%$ rH) without condensation in the sampling lines at any place in the system. Experiments were performed with a cabinet temperature of $37.8\text{ °C} (\pm 0.1\text{ °C})$ that was stable, with the use of 4 additional heating units (Fig. 2 E), and homogenous, using 4 additional ventilation fans for heat distribution in the cabinet. The temperature variation within the exposure modules was $\pm 0.1\text{ °C}$ and was independently maintained by the additional

external water circulation bath. The heated inlet system (Fig. 2 A) enabled a constant aerosol temperature before entering the system and thus helped to have a stable temperature of $37\text{ °C} \pm 0.1\text{ °C}$ at the cellular stage. The constant aerosol temperature revealed to be also important for stable humidification of the aerosol. Humidification of the CA and the aerosol was generated by two humidification units (Fig. 2 D) and was set at $86.5 \pm 1.5\%$ (Fig. 2 C). Short periodic rH drops to 81% can be observed for 5 s in exact 2-h intervals and are caused by the clearing of excess water in the humidification units. Following the modifications, rH fluctuations were less frequent and less pronounced.

- Temperature and rH control at the cellular level: Aerosol temperature and rH at the cellular level were constantly measured by module sensors placed in the clean air and aerosol stages and revealed to be important for long term exposures as there are differences with different sensor placement in the system. The system measures constantly the humidity of the AA/CA with an internal aerosol reactor sensor and an internal CA unit sensor. The comparison of the data recorded by both internal sensors and the newly implemented module sensors revealed that the measured rH at the cellular level (inside the module) was different than the rH measured by the internal humidity sensors: With the same system settings, the measured rH at cellular level was higher in the CA stage and lower in the AA stage (data not shown) compared to the sensors placed in the CA unit and aerosol reactor (Fig. S1). Therefore, the AES settings were adjusted before the start of the cell exposure with the module sensors, to obtain comparable exposure conditions in the aerosol and clean air modules.
- Automation of the system: For increasing the AES autonomy time without operator, an automated water re-fill system (Fig. 2 E) was installed to provide water in hourly intervals to the water circulation baths supplying the humidification units. The volume of the water reservoir (8L) was chosen to allow for >72h constant running of both humidification units without manual re-filling. Additionally, a

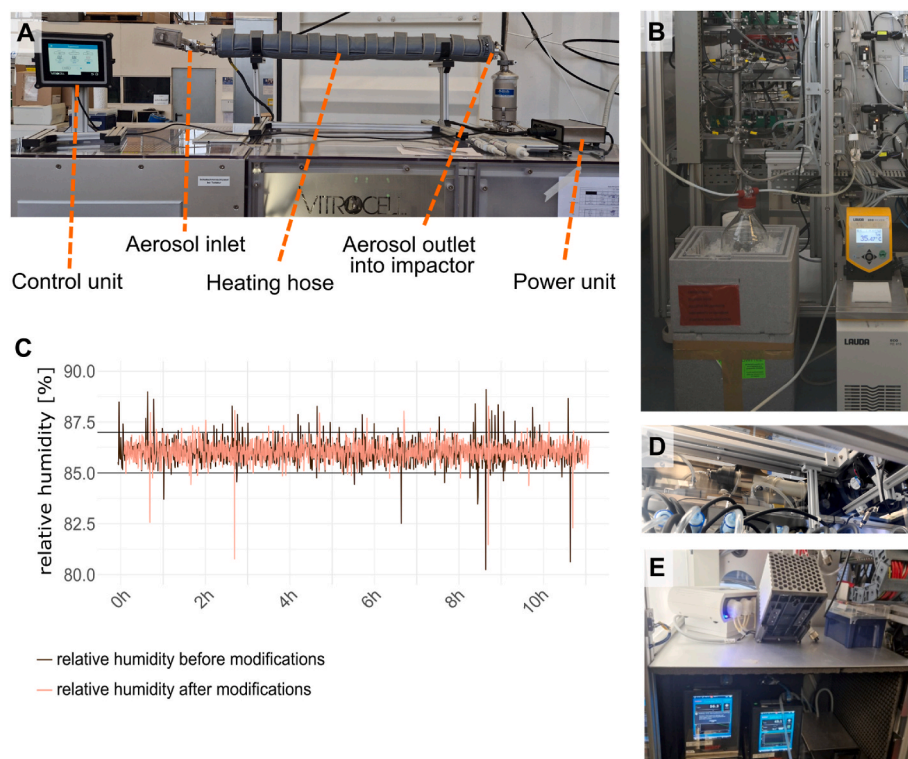


Fig. 2. Adaptations of the AES for long-term exposures. (A) Heated inlet with power supply and control unit. (B) Circulation bath for module temperature and water trap before mass flow controller. (C) Stability of humidity before and after changes over 11h. (D) Humidification unit in separate compartment and horizontally oriented. (E) Refill system of water heater for humidification unit and additional installed heater.

cooled water trap was placed after the reactor in front of the humidity sensitive parts (Fig. 2 B) of the exhaust line.

3.2. Characterization of ambient air during long-term cell exposure

Three independent long-term cell exposures to ambient air were performed in Fall (2022), in the southern part of Munich, in an urban area. The first exposure was performed over a weekend (WE) (Friday to Monday), the second during a working week (WW) (Tuesday to Friday) and the third during a working week (Monday to Thursday) including a

public holiday on the second day (WWH) (Tuesday) (Fig. 3 A). During the WE and at the beginning of the WW exposures, rain was detected (Fig. 3 B). Mean temperatures and mean rH were similar between each exposure with a small decline in temperature from the first to the third exposure (Fig. 3 C and D). Median temperatures $\pm 95\%$ CI decreased from 14.6 ± 0.3 °C, 12.5 ± 0.4 °C, to 11 ± 0.4 °C from the first to the third exposures and rH was on average 85%.

During the WE exposure, the PM_{2.5} mass concentration (4.2 ± 0.1 $\mu\text{g m}^{-3}$) and PNC (median \pm CI: $1.1 \times 10^3 \pm 0.03 \times 10^3$ m^{-3}) were lower compared to WW (6.5 ± 0.1 $\mu\text{g m}^{-3}$ and $3.1 \times 10^3 \pm 0.05 \times 10^3$ m^{-3}

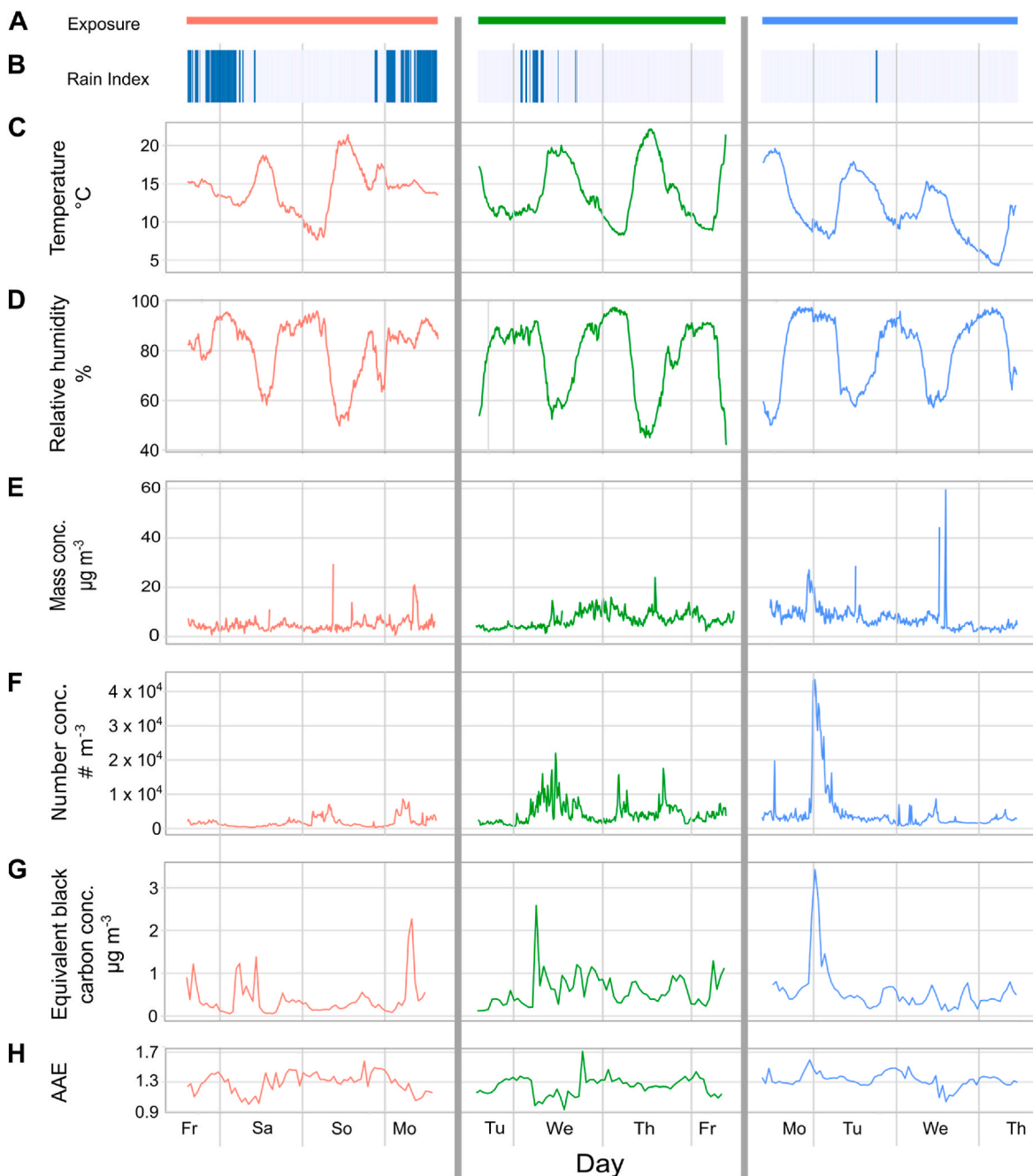


Fig. 3. Physical aerosol characterization of ambient air during cell exposures. (A) Period of exposure: 1) Weekend (WE), in red; 2) Work week (WW) in green; 3) Work week with one holiday (WWH) in blue. (B) Precipitation occurrence index. (C–D) Ambient temperature (°C) and relative humidity (%). Data presented in B, C, and D were measured by the Munich city weather station of the DWD (German weather service) and is illustrated in 10 min averages. (E) Mass concentration ($\mu\text{g m}^{-3}$) measured by the tapered element oscillating microbalance (TEOM) and is illustrated in 10 min averages. (F) Particle number concentration ($\# \text{m}^{-3}$) measured by the condensation particle counter (CPC) in 10 min averages. (G) Equivalent Black Carbon ($\mu\text{g m}^{-3}$) and (H) the corresponding absorption Ångström exponent measured with the aethalometer given in 1h averages. PNC: Particle number concentration, eBC: equivalent black carbon, AAE absorption Ångström exponent. (For interpretation of the references to colour in this figure legend, the reader is referred to the Web version of this article.)

respectively) and WWH ($6.9 \pm 0.1 \mu\text{g m}^{-3}$ and $2.4 \times 10^3 \pm 0.1 \times 10^3 \text{ m}^{-3}$ respectively) exposures (Fig. 3E and F). The ambient air during WWH exposure, which comprised a public holiday, presented a slightly higher mass concentration than the WW exposure but also the highest variability due to a large increase of PNC during the first evening. This large PNC increase was detected by our measurements as well as by a neighboring measuring station of the Bavarian Environmental Agency (Fig. S2).

CO and $\text{PM}_{2.5}$ concentrations were also largely increased during this episode. eBC concentrations (Fig. 3 G) were the lowest during the WE

($0.28 \pm 0.1 \mu\text{g m}^{-3}$) compared to WW and WWH ($0.52 \pm 0.1 \mu\text{g m}^{-3}$ and $0.45 \pm 0.1 \mu\text{g m}^{-3}$ respectively). During the periods of rain, eBC, PNC, mass concentrations, and $\text{PM}_{2.5}$ (Fig. 3, Fig. S2) were significantly decreased due to wet deposition (Andronache, 2004b; Wang et al., 2014). However, there were no significant differences in the average AAE calculated in all three periods, which was approximately of 1.3.

Evaluation of the chemical composition with an untargeted GC \times GC-MS approach revealed a complex aerosol composition with similar compound groups in variable concentrations between the different exposure periods (Fig. 4A and B). As PAHs and hopanes are

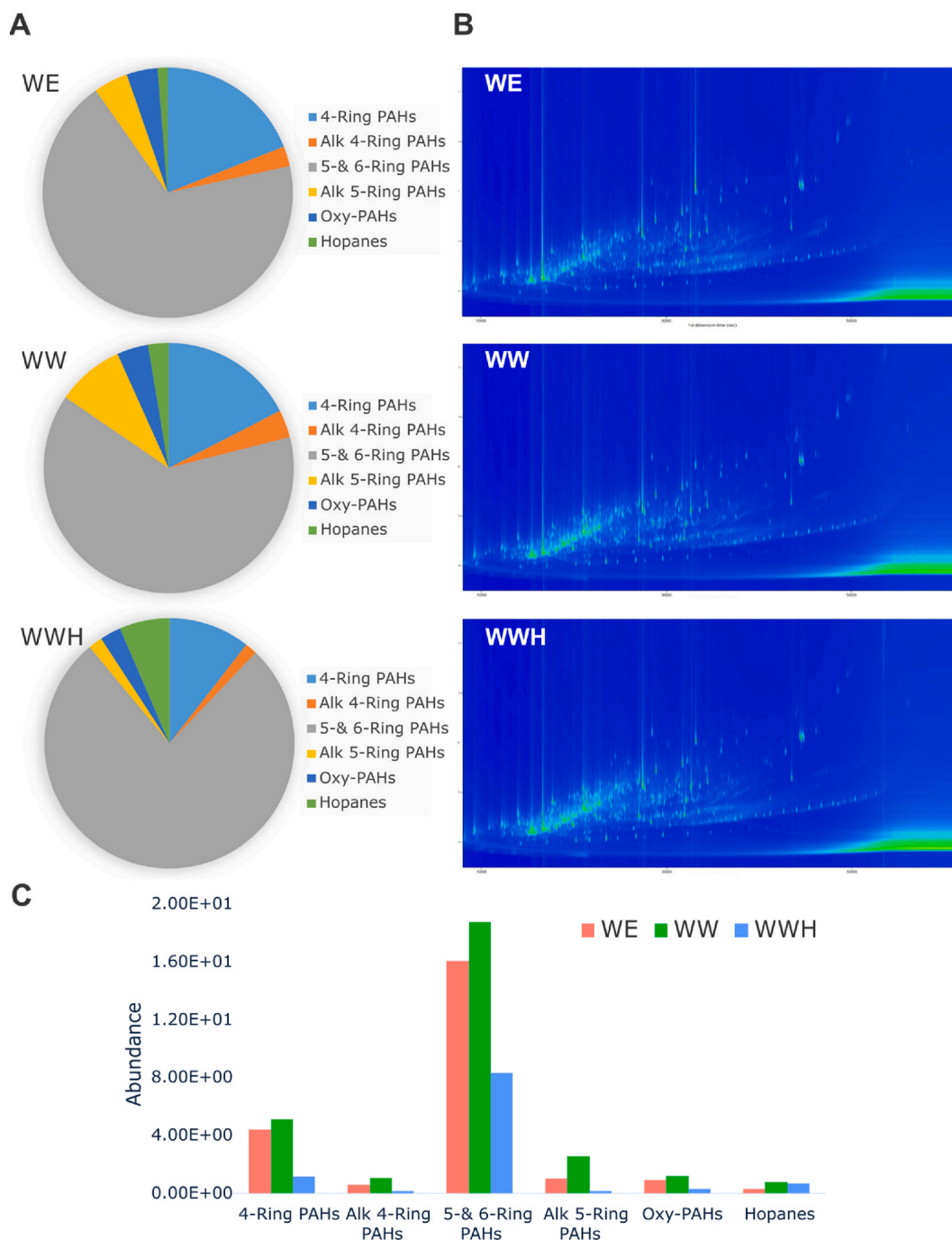


Fig. 4. Non-targeted determination of the PM samples conducted by direct thermal desorption comprehensive two-dimensional gas chromatography time-of-flight mass spectrometry (DTD-GC \times GC-TOFMS). (A) Pie-charts of the area percentage of each class within each sample. (B) Two-dimensional chromatograms from the three 72h samples. (C) Abundance/Area (normalized to d12-Benz(e)pyrene) of different compound classes with potential health related effects for the three different samples. Alk – alkylated; Oxy – oxygenated. 1) Weekend (WE), in red; 2) Work week (WW) in green, 3) Work week with one holiday (WWH) in blue. (For interpretation of the references to colour in this figure legend, the reader is referred to the Web version of this article.)

toxicologically relevant compound classes and they are omnipresent in ambient air samples, a classification of PAHs and hopanes was conducted. From those classified peaks, the most abundant classes were 5- & 6-Ring PAHs (64–78%) followed by the smaller 4-Ring PAHs (11–19%). Alkylated 5-Ring PAHs were most present and in slightly higher proportion during the WW (9%) compared to WE and WWH (respectively 4% and 2%). A similar trend was shown for alkylated 4-Ring PAHs, although not as pronounced with values ranging from 2 to 4% and oxygenated PAHs had similar values in all exposures with 3–4% (Fig. 4 A). During the WWH exposure, we could detect the biggest fraction of 5- & 6-Ring PAHs (78%) as well as the biggest fraction of hopanes (7%) compared to the WW (3%) and especially the WE exposure (1%). By normalizing the detected area to the internal standard benz[e]pyrene-d12, the abundances of the detected classes were estimated (Fig. 4 C). The highest amounts were estimated for WW followed by the WE and the least at the WWH. This was shown for all compound classes, except for hopanes, which were detected in higher proportion during WWH compared to WE. Comparing the WW and the WE exposures, the estimated abundance increase of detected compound classes ranged from 1.2-fold (4-Ring PAHs) to 2.6-fold (Hopanes) but was more pronounced between WW and WWH, ranging from 1.1-fold (Hopanes) to 13.1-fold (alkylated 5-Ring PAHs).

To confirm the abundance estimates, determination of 12 of the 16 designated High Priority PAHs by the Environmental Protection Agency (EPA) (Hussar et al., 2012) was performed and showed similar results (Table 2, Fig. S3). The same PAHs were detected in all exposures, with higher amounts during the WW and WE compared to the WWH. In general, we could observe 8% more analyzed PAHs during the WW compared to the WE and 6.7% more compared to the WWH. These included also known carcinogenic (benz[a]pyrene) and possibly carcinogenic compounds (benz[a]anthracene, benzo[b,j & k]fluoranthene, chrysene, indeno[1,2,3-cd]pyrene) according to the classification of the IARC (IARC, 2010).

3.3. Epithelial integrity and cellular toxicity evaluation after long-term ambient air exposure in Calu-3 cells

Cellular toxicity and epithelial integrity were not different between incubator control and clean air exposed cells (Fig S4 A-C, Fig. S5), hence we compared the biological responses induced by ambient air (AA) to the clean air (CA) controls. Epithelial integrity was maintained during the 72 h exposures with an increase of dead cells with AA compared to CA exposed cells (Fig. 5 A). Long-term AA exposures induced a significant but small increase in cytotoxicity compared to CA in all exposures (Fig. 5 B). The increase in cytotoxicity was largest during WW (3.3%) followed by WWH and WE (respectively 2.3% and 2.0%). Additionally, the metabolic activity of Calu-3 cells was indicated to decrease slightly with AA compared to CA exposure with the same trend (Fig. 5 C).

Table 2

Quantification of relevant PAHs (ng m⁻³) on filter samples after 24h sampling (0.9 m³). PAH: Polycyclic Aromatic Hydrocarbons; WE: Weekend; WW: Work Week; WWH: Work Week with one Holiday.

| PAHs | WE | | | | WW | | | | WWH | | | |
|--------------------------------|-------|-------|-------|------|-------|-------|-------|------|-------|-------|-------|------|
| | Fr-Sa | Sa-Su | Su-Mo | mean | Tu-We | We-Th | Th-Fr | mean | Mo-Tu | Tu-We | We-Th | mean |
| Fluoranthene | 1.0 | 0.1 | 0.3 | 0.5 | 1.0 | 0.3 | 0.8 | 0.7 | 0.2 | 0.2 | 0.1 | 0.2 |
| Pyrene | 2.6 | 0.1 | 0.6 | 1.1 | 2.2 | 0.4 | 1.4 | 1.3 | 0.3 | 0.2 | 0.2 | 0.2 |
| Benz [a] anthracene | 1.3 | 0.0 | 0.6 | 0.6 | 1.7 | 0.3 | 0.8 | 0.9 | 0.1 | 0.1 | 0.1 | 0.1 |
| Chrysene | 2.1 | 0.0 | 1.2 | 1.1 | 3.1 | 0.4 | 1.4 | 1.6 | 0.2 | 0.1 | 0.1 | 0.1 |
| sum Benzo [b,j,k] fluoranthene | 7.2 | 0.2 | 3.0 | 3.4 | 5.8 | 2.0 | 2.9 | 3.5 | 0.9 | 0.4 | 0.4 | 0.6 |
| Benz [e] pyrene | 3.0 | 0.1 | 1.3 | 1.4 | 2.3 | 0.8 | 1.1 | 1.4 | 0.4 | 0.2 | 0.2 | 0.2 |
| Benz [a] pyrene | 3.4 | 0.0 | 1.3 | 1.5 | 2.9 | 0.6 | 1.3 | 1.6 | 0.3 | 0.2 | 0.1 | 0.2 |
| Perylene | 0.7 | 0.0 | 0.3 | 0.3 | 0.7 | 0.1 | 0.2 | 0.4 | 0.1 | 0.0 | 0.0 | 0.0 |
| Indeno [1,2,3-cd] pyrene | 1.7 | 0.1 | 0.7 | 0.8 | 1.2 | 0.5 | 0.6 | 0.7 | 0.2 | 0.1 | 0.1 | 0.1 |
| Dibenz [ah] anthracene | 0.3 | 0.0 | 0.0 | 0.1 | 0.1 | 0.1 | 0.0 | 0.1 | 0.0 | 0.0 | 0.0 | 0.0 |
| Benzo [ghi] perylene | 3.0 | 0.1 | 1.2 | 1.4 | 2.0 | 0.8 | 0.9 | 1.2 | 0.4 | 0.2 | 0.2 | 0.2 |
| Coronene | 1.4 | 0.0 | 0.5 | 0.6 | 0.9 | 0.3 | 0.3 | 0.5 | 0.2 | 0.1 | 0.1 | 0.1 |

Statistical evaluation of metabolic activity indicated in all three exposures significant decreases, but were not as such counted, as there was not always a $n \geq 3$. Though not significant, AA decreased the metabolic activity of the bronchial epithelial cells by 7.2% (WW) to 5.1% (WE). Between the CA exposed Calu-3 cells and the Inc, no significant differences in LDH release or number of dead cells could be observed, indicating no additional effect due to constant exposure in Calu-3 cells for 72 h (Fig S 4 A, C). Although cytotoxicity and metabolic activity illustrated differences between AA and CA exposed Calu-3 cells, no difference was observed with the TEER measurements comparing AA and CA (Fig. 5 D), indicating no perturbation of tight junction dynamics integrity. This result is also supported by microscopical analysis of the tight junctions by ZO-1 staining, in all conditions (Fig. S5).

3.4. Biological responses and molecular changes of Calu-3 cells after long-term exposure

Proinflammatory and oxidative stress responses of the bronchial epithelial cells were assessed after exposure to ambient air by evaluating the release of two cytokines IL-6 and IL-8, as well as the release of MDA, a marker of lipid peroxidation. Release of pro-inflammatory cytokines IL-6 and IL-8 did not show a distinct difference between AA and CA exposed cells (Fig. 5 E and F). Fig. 5 G displays the MDA release, as an oxidative stress indicator. Although we could not detect significant differences between AA and CA, AA exposure slightly increase MDA release in Calu-3 cells.

Fig. 6 displays the changes in the expression of genes involved in different cellular mechanisms. The gene expression (in fold change) of pro-inflammatory marker genes *CXCL8* (IL-8) and *TLR2* indicates no distinct difference between AA and CA exposed Calu-3 cells. On the other hand, cells exposed to AA induced a downregulation of *IL-6* compared to their CA controls for WE and WW. AA induced an *IL-6* downregulation during WW and WE compared to CA. The gene expression of the pro-inflammatory marker gene *IL1B* was increased after all AA exposures compared to CA. Expression fold change of *IL1B* was 1.5-fold higher compared to CA during WW or WE and WWH caused a fold change increase of 1.8. Cells exposed to AA during WE and WW exposures presented an increased *CYP1A* and *CYP1B1* gene expression compared to their respective CA controls. Except for a small decrease during WE, no modulation of the gene expression of the oxidative stress marker gene *HMOX1* was induced by AA compared to CA for all exposures.

4. Discussion

Our study aimed to investigate the effects of continuous 72 h exposure to ambient air pollution on human bronchial epithelial cells using an automated exposure system adapted for *in vitro* long-term exposures.

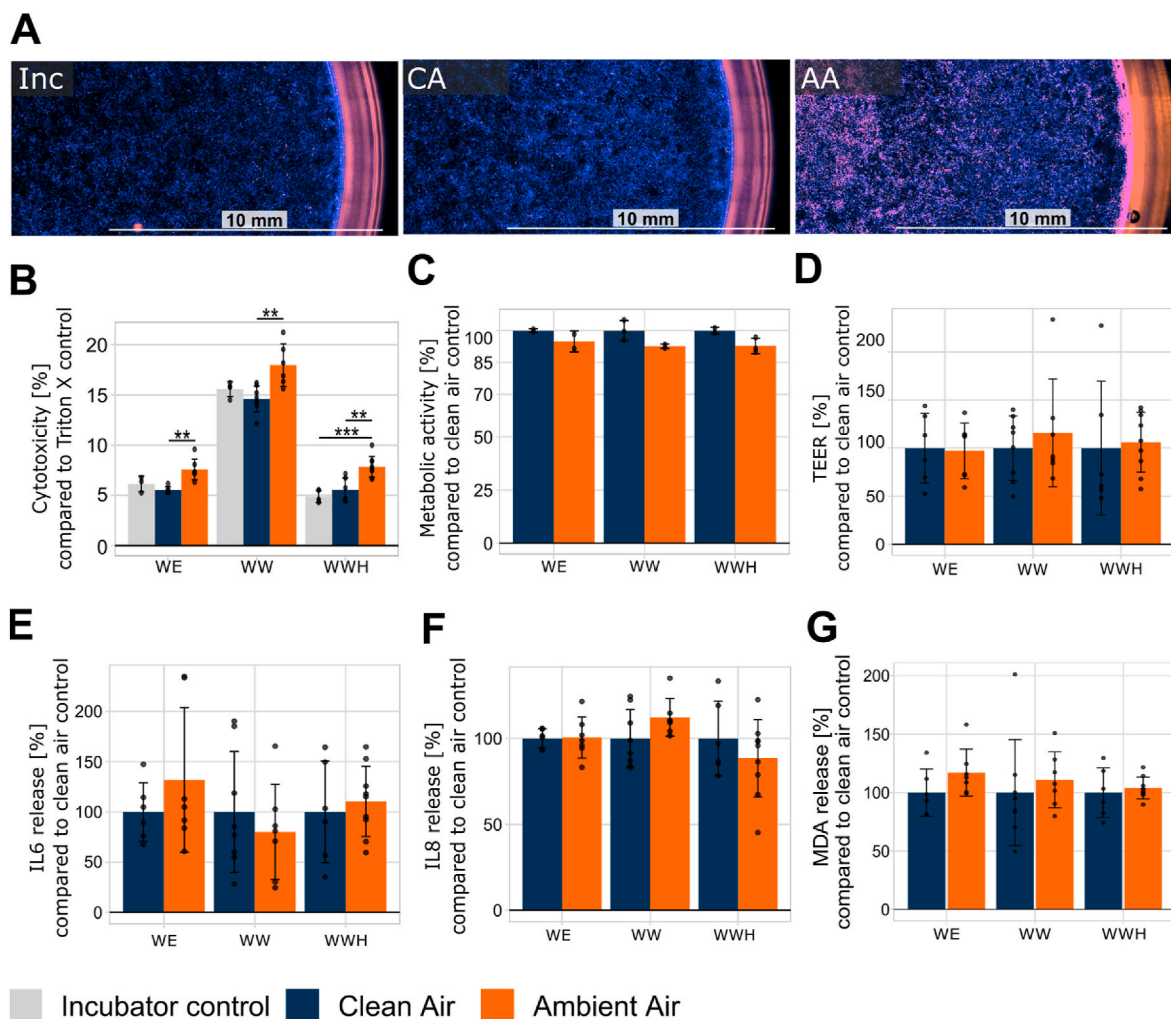


Fig. 5. Toxicity assessment of long-term ambient air exposure in Calu-3 cells at ALI. Calu-3 cells were exposed to ambient air or clean air. (A) Representative live/dead cell imaging with 5 $\mu\text{g mL}^{-1}$ H 33342 nuclei stain (blue) and 2.5 $\mu\text{g mL}^{-1}$ propidium iodide (orange) to selectively stain dead cells after 72h exposure in the different exposure/control settings. (B) Percentage cytotoxicity measured by LDH assay and normalized to clean air control. (C) Metabolic activity was measured by resazurin assay and normalized to clean air control. (D) Cell layer integrity was measured by TEER measurements and normalized to clean air control. (E) IL-6 and (F) IL-8 release of Calu-3 cells normalized and compared to respective CA control. (G) MDA of Calu-3 cells normalized and compared to respective CA control and assessed by liquid chromatography tandem mass spectrometry measurements. Data is shown as mean \pm SD in bars, and $n \geq 3$ for B and D, $n \geq 0.2$ in C, $n \geq 6$ in E, F, G. Each biological replicate (one insert) is indicated with a dot. Significances are shown in comparison to the respective clean air or Inc control (analysis via *t*-test when $n \geq 3$. ** $p \leq 0.01$, *** $p \leq 0.001$). WE: weekend, WW: work week, WWH: work week with one holiday, CA: clean air, AA: ambient air, TEER: transepithelial electrical resistance. (For interpretation of the references to colour in this figure legend, the reader is referred to the Web version of this article.)

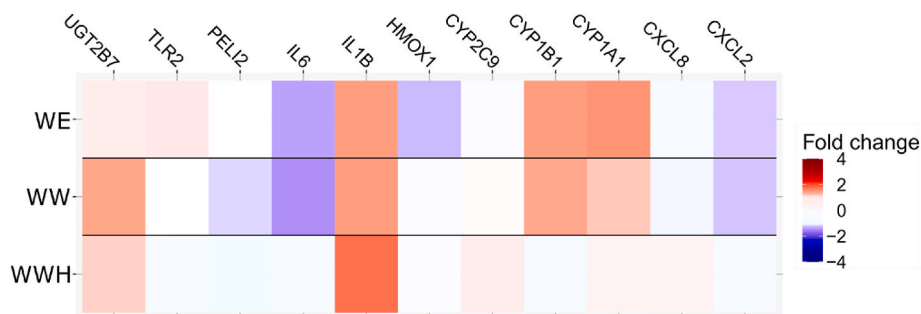


Fig. 6. Gene expression evaluation after long-term ambient air exposure of Calu-3 cells at ALI. Calu-3 cells were exposed to ambient air (AA) or clean air (CA). Gene expression fold change of (A) inflammatory (CXCL2, CXCL8, IL1B, IL6, PELI, TLR2, UGT2B7), (B) Xenobiotic (CYP1A1, CYP1B1, CYP2C9) and oxidative stress (HMOX1) related marker genes. Expression fold change is normalized to two housekeeping genes (GAPDH, RFLP13A) and compared to CA control. Data are shown as mean ($n = 2-4$). Detailed information is available in Table S 1. WE: weekend, WW: work week, WWH: work week with one holiday.

We found that the adapted AES system is capable of stable 72 h ambient air exposures and provides the sensitivity to observe cellular responses of Calu-3 cells exposed to ambient air pollution concentrations, indicated by cytotoxicity and differential gene expression.

To enable long-term cell exposure, the aerosol exposure system had to fulfil specific requirements to ensure stable operations as well as optimal conditions for the cells. These included a decreased air flow from 100 mL min^{-1} to 50 mL min^{-1} in comparison to previous studies (Oeder et al., 2015; Zimmermann et al., 2023) to avoid long-term induced cellular shear stress. In addition, we observed that pre-conditioning of the aerosol is important to have stable temperature and rH conditions of the aerosol as it was indicated in previous studies (Binder et al., 2022; Zavala et al., 2017). Moreover, using the module sensors for calibration and subsequently the new online monitoring tool for observation allowed for similar start conditions in the CA and AA stages and the option to observe and fine tune during the long-term exposure with remote access. In a recent study, it has been postulated, that for obtaining meaningful results, it is essential to comprehensively characterize the effect of the exposure system on the cell model system, compared to an additional control (Buckley et al., 2024). Similarly to this study, we compared our clean air controls with the incubator controls. We observed no difference in epithelial integrity (Fig S4 B), cellular toxicity (Fig S5 A, C) and IL-6 release between the unexposed (Inc) and clean air exposed cells. However, significant changes in IL-8 and MDA release were detected, and although it is possibly influenced by the constant air flow over the cells (Buckley et al., 2024), the long exposure duration of 72 h can create varying degradation conditions for released cytokines. It has already been shown, that 6–10 h storage of blood samples at RT, lead to significant degradation of cytokines (Cohen et al., 2019), which likely also takes place during 72 h exposure at 37°C and hence makes the interpretation of sensitive cytokine release measurements difficult. Evaluation of released cytokines poses a challenge for long term exposures and requires further replicates or online measurements to also account for degradation.

In previous studies with similar systems from our and other groups, exposure durations of 1–4 h are usually performed (Bessa et al., 2021; Candeias et al., 2022; Delaval et al., 2022; Dilger et al., 2023; Jonsdottir et al., 2019; Oeder et al., 2015; Offer et al., 2022; Pantzke et al., 2023; Zimmermann et al., 2023) or repeated exposures of 4 h or 12 h per day (Bisig et al., 2018; Braakhuis et al., 2020). The longer continuous exposure duration allowed to reduce the test compound dose at realistic concentrations or even the direct exposure of human lung cells to ambient air (Bisig et al., 2018; Gualtieri et al., 2018).

The choice of lung cell model is of pivotal importance for long-term exposures. This study utilized a single cell line to ensure experimental consistency and reproducibility, while providing a well-characterized model relevant to the normal human bronchial epithelium. At ALI, Calu-3 cells form and maintain a homogenous epithelial monolayer, form tight junctions, withstand the airflow, and can be cultivated for weeks (Braakhuis et al., 2020). We could confirm the properties of the Calu-3 cells, we did not detect differences between CA exposed and Incubator control cells, even with constant airflow in the system which is not present in the incubator. In a similar setting, BEAS-2B cells were exposed to ambient air (Gualtieri et al., 2018), but only up to 24 h, as BEAS-2B cells, compared to Calu-3 cells, do not form such a robust monolayer with secretory and ciliated cell phenotypes and have limited differentiation capacity (Ehrhardt et al., 2008; Stewart et al., 2012). The robustness of Calu-3 cells enables their use in assessing heavily polluted environments with for instance very high concentrations of $\text{PM}_{2.5}$. Human health risk from exposures in workshops, construction sites or industrial cities in India and China could be systematically evaluated.

Ambient air exposure for 72 h caused a significant increase in cytotoxicity in all tested exposures to ambient air, indicated decrease in metabolic activity, but no epithelial integrity loss or pro-inflammatory cytokine release. In many previous studies and reviews, *in vitro* cytotoxicity has been attributed to different organic aerosols and gases

(Binder et al., 2021; Gan et al., 2020; Juarez Facio et al., 2022; Kelly and Fussell, 2012; Moreno-Ríos et al., 2022). These studies focused on single sources and concentrations which were set much higher than realistic concentrations to mimic in a short amount of time much longer periods. Interestingly, studies investigating the combined effect of two different compounds or sources reported attenuated cellular responses (Candeias et al., 2022; Clifford et al., 2017; Zimmermann et al., 2023) and increased toxicity even at very low doses (Forest, 2021; Jiang et al., 2020). However, in our study, the exposure to complex mixture of ambient air could explain the low but significant cytotoxicity observed in our study, even though cells were exposed to low environmental concentrations. Similar cytotoxicity increase was found by Bisig et al. (2018) in 16HBE14o-bronchial epithelial cells repeatedly exposed to ambient air for $3 \times 12\text{h}$ (12h/day). A recent cohort study by Weichenhal et al. (2022) indicated that even at very low levels of outdoor $\text{PM}_{2.5}$, there were 1.5 million additional attributable death each year globally, further highlighting the impact and importance of studying air pollutants at very low doses.

Interestingly, while we could not observe differences in IL-6 or IL-8 release by bronchial epithelial cells exposed to ambient air compared to clean air, neither in *CXCL8* gene expression, there was a slight down regulation of IL-6 gene expression in cells exposed to AA during WE and WW exposures compared to CA exposed cells. Gene expression studies on Calu-3 cells are scarce, but previous studies working with bronchial epithelial lung cells BEAS-2B reported a down regulation of *CXCL8* and, similar to our study, *IL6* following UFP or particulate matter emission exposure at the ALI or submerged (Ahmed et al., 2020; Juarez Facio et al., 2022). In the study of Ahmed et al. (2020) it was reported that *IL6* downregulation is connected and mediated by PAHs, indicating the possible link between PAHs and the negative regulation of inflammatory response. This could explain our observations that the slight down-regulation of *IL6* gene expression is more pronounced with increasing PAH concentrations (Fig. 7). On the other hand, we observed an indication for upregulation of the proinflammatory marker *IL1 β* in cells exposed to AA in all exposure periods and the xenobiotic marker genes *CYP1A1* as well as *CYP1B1* following AA exposure during WE and WW possibly induced by higher PAH concentration. Similar observations were made in a previous study, where *CYP1B1* was induced in mice lung and liver by PAHs (e.g. B[a]P, 7,12-dimethylbenz[a]anthracene, dibenz[a,l]pyrene, 3-methylcholanthrene, 1,2,5,6-dibenzanthracene, benzo[b]fluoranthene, and benzo[a]anthracene), via the aryl hydrocarbon receptor (Shimada et al., 2002). By linking differential gene expression of CYP enzymes, which are involved in xenobiotic metabolism, with exposure to pollutants like $\text{PM}_{2.5}$ and benz[a]pyrene, our study enhances the scientific basis for evaluating the long-term health risks associated with urban air pollution, even at low levels.

The physical and chemical characterization of the ambient air revealed air pollution concentrations of low levels within the legal limits. $\text{PM}_{2.5}$ concentrations ranged between $7 \mu\text{g m}^{-3}$ during the WE to $12 \mu\text{g m}^{-3}$ during the WW and were thus below the German limit of $25 \mu\text{g m}^{-3}$ (BImSchV, 2016), but above the $5 \mu\text{g m}^{-3}$ recommended by WHO (WHO, 2021b). This recommended value was recently reduced from $10 \mu\text{g m}^{-3}$ to $5 \mu\text{g m}^{-3}$, based on epidemiological studies indicating additional mortality caused by $\text{PM}_{2.5}$ levels below $10 \mu\text{g m}^{-3}$ (Stafoggia et al., 2022; Strak et al., 2021; Weichenhal et al., 2022). Regarding PAH concentrations, only benz[a]pyrene has currently a recommendation in the EU with a target of 1 ng m^{-3} (annual mean). Detected concentrations during the exposure periods in our study were higher than the recommendation with a 24 h mean of up to 3.4 ng m^{-3} . The Toxic Equivalency Factors (TEF) calculation revealed that the two first exposure periods (WE and WW) showed similar TEQ of 2.3 ng m^{-3} which were 7 times higher than during the third period (WWH: 0.3 ng m^{-3}), potentially indicating higher human health risk due to exposure to PAH in ambient air (Jung et al., 2010; Ohura et al., 2005). Given the global burden of air pollution-related diseases, our study underscores the need to reduce human exposure to environmental air pollutants, particularly in urban

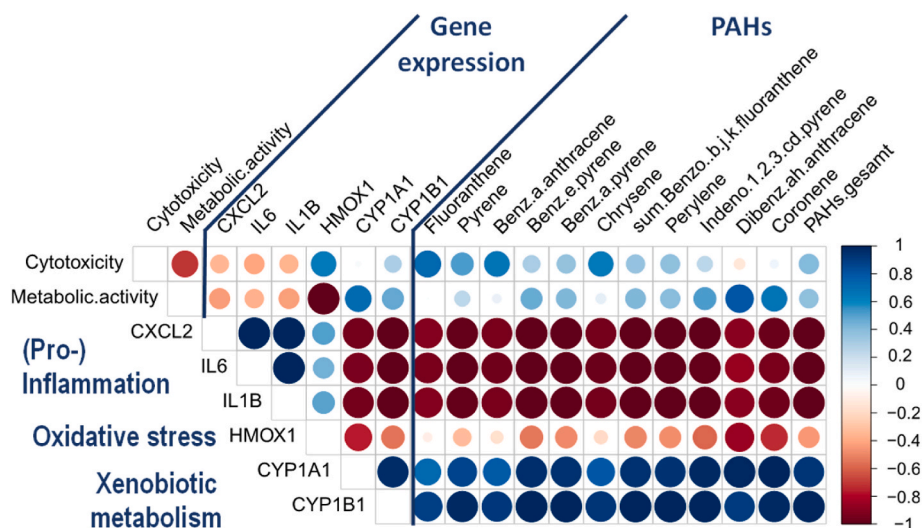


Fig. 7. Correlation matrix of differential gene expression of selected genes and polycyclic aromatic hydrocarbon content. Pearson correlation coefficient was calculated. Positive correlations are indicated in blue and negative correlations are indicated in red. PAH: Polycyclic aromatic hydrocarbon.

settings, to protect respiratory and overall public health.

In vitro long-term exposures to ambient air could provide compelling toxicological data for evaluating the human health risk at certain locations, like workplaces or highly polluted cities, by combining specific biomarkers and physicochemical characterization. However, there are also limitations. Due to the complexity of the ambient air and endless possibilities on how different compounds interact with each other as well as with human cells, this approach is limited to studying the effects of the mixture of aerosol and the cellular mechanisms involved. For the risk assessment of single compound, single source exposures are still needed. Another limitation of our study is the parameters of the clean air control. To further improve the system, CO₂ should be added to the CA, making it more realistic and comparable to ambient air. Moreover, due to the long exposure time, the number of timepoints is limited, making it more difficult to directly correlate cellular responses to the physical and chemical characteristics which vary strongly in ambient air. The use of online aerosol characterization instruments like the scanning mobility particle sizer (SMPS) can also be considered for further studies as particle size is an important parameter and can be used for estimating the size-dependent particle deposition on the ALI epithelial cell layer (Lucci et al., 2018). Furthermore, due to the long exposure time and limitation in sample number, the number of replicates needs to be carefully considered, to fit into the system while adjusting for the biological variance. Thus, further studies are needed with the possibility to sample or to monitor online biomarkers of interest throughout the duration of the exposure without influencing the exposed cells. This study was also limited due to the use of a single cell line, and we therefore recommend the use of co-culture models comprising immune cells and/or fibroblasts for instance, or the use of primary cells for further improving the sensitivity of the *in vitro* model without losing its robustness, and mimic closer the complexity of the human airways.

5. Conclusion

We demonstrated that long-term aerosol *in vitro* exposures at the ALI are feasible, providing a significant step toward realistic risk assessment for indoor and outdoor environments. Direct exposure to ambient air resulted in cytotoxicity and changes in the gene expression of inflammation-related genes in a bronchial epithelial monoculture cell model. Future efforts will focus on integrating the adapted AES with more complex co-culture systems, such as Calu-3 cells combined with human derived macrophages, to better evaluate the underlying cellular mechanisms in air pollutant exposure. This approach could be extended

to diverse occupational and private environments, offering valuable insights for developing effective risk assessment strategies. Overall, our work establishes a comprehensive method for evaluating the long-term toxicity of ambient air and reinforces the need for strategies to mitigate air pollution's impact on human health.

CRedit authorship contribution statement

E.J. Zimmermann: Writing – review & editing, Writing – original draft, Visualization, Investigation, Formal analysis, Data curation, Conceptualization. **A. Das:** Writing – review & editing, Writing – original draft, Visualization, Investigation, Formal analysis, Conceptualization. **A. Huber:** Writing – review & editing, Writing – original draft, Methodology, Investigation, Formal analysis. **N. Gawlitta:** Writing – review & editing, Visualization, Investigation, Formal analysis. **E. Kuhn:** Writing – review & editing, Investigation. **C. Schlager:** Writing – review & editing, Validation, Methodology, Conceptualization. **B. Gutmann:** Writing – review & editing, Methodology, Funding acquisition. **T. Krebs:** Writing – review & editing, Validation, Resources, Methodology, Funding acquisition, Conceptualization. **J. Schnelle-Kreis:** Writing – review & editing, Supervision, Conceptualization. **M.N. Delaval:** Writing – review & editing, Writing – original draft, Visualization, Supervision, Project administration, Investigation, Formal analysis, Data curation, Conceptualization. **R. Zimmermann:** Writing – review & editing, Supervision, Resources, Funding acquisition, Conceptualization.

Funding

This study was funded by the Bundesministerium für Wirtschaft und Klimaschutz (BMWK) Zentrales Innovationsprogramm Mittelstand (ZIM) (grant number 16KN083620, Feinstaub-Clean Air - Alias Lung), and was partially financed by the Helmholtz International Laboratory aeroHEALTH (InterLabs-0005), and Helmholtz Virtual Institute of Complex Molecular Systems in Environmental Health - Aerosols and Health (HICE). Nadine Gawlitta and Anusmita Das acknowledge financial support by the Bavarian State Ministry of the Environment and Consumer Protection.

Declaration of competing interest

The authors declare the following financial interests/personal relationships which may be considered as potential competing interests:

Christoph Schlager reports financial support was provided by Vitrocell Systems GmbH. Bastian Gutmann reports financial support was provided by Vitrocell Systems GmbH. Tobias Krebs reports financial support was provided by Vitrocell Systems GmbH. If there are other authors, they declare that they have no known competing financial interests or personal relationships that could have appeared to influence the work reported in this paper.

Appendix A. Supplementary data

Supplementary data to this article can be found online at <https://doi.org/10.1016/j.envres.2025.120759>.

Data availability

Data will be made available on request.

References

- Aguilera, I., Dratva, J., Caviezel, S., Burdet, L., de Groot, E., Ducret-Stich, R.E., Eeftens, M., Keidel, D., Meier, R., Perez, L., Rothe, T., Schaffner, E., Schmit-Trucksass, A., Tsai, M.Y., Schindler, C., Kunzli, N., Probst-Hensch, N., 2016. Particulate matter and subclinical atherosclerosis: associations between different particle sizes and sources with carotid intima-media thickness in the SAPALDIA study. *Environ. Health Perspect.* 124 (11), 1700–1706. <https://doi.org/10.1289/EHP161>.
- Ahmed, C.M.S., Yang, J., Chen, J.Y., Jiang, H., Cullen, C., Karavalakis, G., Lin, Y.H., 2020. Toxicological responses in human airway epithelial cells (BEAS-2B) exposed to particulate matter emissions from gasoline fuels with varying aromatic and ethanol levels. *Sci. Total Environ.* 706, 135732. <https://doi.org/10.1016/j.scitotenv.2019.135732>.
- Bessa, M.J., Brandao, F., Fokkens, P.H.B., Leseman, D., Boere, A.J.F., Cassee, F.R., Salmatoniadis, A., Viana, M., Vulpoi, A., Simon, S., Monfort, E., Teixeira, J.P., Fraga, S., 2021. In vitro toxicity of industrially relevant engineered nanoparticles in human alveolar epithelial cells: air-liquid interface versus submerged cultures. *Nanomaterials* 11 (12). <https://doi.org/10.3390/nano11123225>.
- BImSchV, 2016. *Verordnung zur Durchführung des Bundes-Immissionsschutzgesetzes*, p. 39.
- Binder, S., Cao, X., Bauer, S., Rastak, N., Kuhn, E., Dragan, G.C., Monse, C., Ferron, G., Breuer, D., Oeder, S., Karg, E., Sklorz, M., Di Bucchianico, S., Zimmermann, R., 2021. In vitro genotoxicity of dibutyl phthalate on A549 lung cells at air-liquid interface in exposure concentrations relevant at workplaces. *Environ. Mol. Mutagen.* 62 (9), 490–501. <https://doi.org/10.1002/em.22464>.
- Binder, S., Rastak, N., Karg, E., Huber, A., Kuhn, E., Dragan, G.C., Monse, C., Breuer, D., Di Bucchianico, S., Delaval, M.N., Oeder, S., Sklorz, M., Zimmermann, R., 2022. Construction of an in vitro air-liquid interface exposure system to assess the toxicological impact of gas and particle phase of semi-volatile organic compounds. *Toxics* 10 (12). <https://doi.org/10.3390/toxics10120730>.
- Bisig, C., Petri-Fink, A., Rothen-Rutishauser, B., 2018. A realistic in vitro exposure revealed seasonal differences in (pro-)inflammatory effects from ambient air in Fribourg, Switzerland. *Inhal. Toxicol.* 30 (1), 40–48. <https://doi.org/10.1080/08958378.2018.1441926>.
- Braakhuis, H.M., He, R., Vandebriel, R.J., Gremmer, E.R., Zwart, E., Vermeulen, J.P., Fokkens, P., Boere, J., Gosens, I., Cassee, F.R., 2020. An air-liquid interface bronchial epithelial model for realistic, repeated inhalation exposure to airborne particles for toxicity testing. *J. Vis. Exp.* 159. <https://doi.org/10.3791/61210>.
- Bredeck, G., Dobner, J., Stahlmecke, B., Fomba, K.W., Herrmann, H., Rossi, A., Schins, R. P., 2023. Saharan dust induces NLRP3-dependent inflammatory cytokines in an alveolar air-liquid interface co-culture model. *Part. Fibre Toxicol.* 20 (1), 39.
- Brook, R.D., Rajagopalan, S., Pope 3rd, C.A., Brook, J.R., Bhatnagar, A., Diez-Roux, A.V., Holguin, F., Hong, Y., Luepker, R.V., Mittleman, M.A., Peters, A., Siscovick, D., Smith Jr., S.C., Whitset, L., Kaufman, J.D., American Heart Association Council on, E., Prevention, C. o. t. K. i. C. D., Council on Nutrition, P. A., & Metabolism, 2010. Particulate matter air pollution and cardiovascular disease: an update to the scientific statement from the American Heart Association. *Circulation* 121 (21), 2331–2378. <https://doi.org/10.1161/CIR.0b013e3181d8e1>.
- Brunkreef, B., Beelen, R., Hoek, G., Schouten, L., Bausch-Goldbohm, S., Fischer, P., Armstrong, B., Hughes, E., Jerrett, M., van den Brandt, P., 2009. Effects of long-term exposure to traffic-related air pollution on respiratory and cardiovascular mortality in The Netherlands: the NLCS-AIR study. *Res. Rep. Health Eff. Inst.* 139, 5–71 discussion 73–89. <https://www.ncbi.nlm.nih.gov/pubmed/19554969>.
- Buckley, A., Guo, C., Laycock, A., Cui, X., Belinga-Desaunay-Nault, M.-F., Valsami-Jones, E., Leonard, M., Smith, R., 2024. Aerosol exposure at air-liquid-interface (AE-ALD) in vitro toxicity system characterisation: particle deposition and the importance of air control responses. *Toxicol. Vitro* 100, 105889.
- Bulus, M., 2023. *Pwrss: statistical power and sample size calculation tools*. R Package Version 0.3.1.
- Candeiias, J., Zimmermann, E.J., Bisig, C., Gawliotta, N., Oeder, S., Groger, T., Zimmermann, R., Schmidt-Weber, C.B., Buters, J., 2022. The priming effect of diesel exhaust on native pollen exposure at the air-liquid interface. *Environ. Res.* 211, 112968. <https://doi.org/10.1016/j.envres.2022.112968>.
- Cho, C.-C., Hsieh, W.-Y., Tsai, C.-H., Chen, C.-Y., Chang, H.-F., Lin, C.-S., 2018. In vitro and in vivo experimental studies of PM_{2.5} on disease progression. *Int. J. Environ. Res. Publ. Health* 15 (7), 1380.
- Clifford, R.L., Jones, M.J., MacIsaac, J.L., McEwen, L.M., Goodman, S.J., Mostafavi, S., Kobor, M.S., Carlsten, C., 2017. Inhalation of diesel exhaust and allergen alters human bronchial epithelium DNA methylation. *J. Allergy Clin. Immunol.* 139 (1), 112–121. <https://doi.org/10.1016/j.jaci.2016.03.046>.
- Cohen, J., 2013. *Statistical Power Analysis for the Behavioral Sciences*. routledge.
- Cohen, L., Keegan, A., Melanson, S.E., Walt, D.R., 2019. Impact of clinical sample handling and processing on ultra-low level measurements of plasma cytokines. *Clin. Biochem.* 65, 38–44.
- Das, A., Pantzke, J., Jeong, S., Hartner, E., Zimmermann, E.J., Gawliotta, N., Offer, S., Shukla, D., Huber, A., Rastak, N., 2024. Generation, characterization, and toxicological assessment of reference ultrafine soot particles with different organic content for inhalation toxicological studies. *Sci. Total Environ.* 951, 175727.
- Decker, T., Lohmann-Matthes, M.-L., 1988. A quick and simple method for the quantitation of lactate dehydrogenase release in measurements of cellular cytotoxicity and tumor necrosis factor (TNF) activity. *J. Immunol. Methods* 115 (1), 61–69.
- Delaval, M.N., Jonsdottir, H.R., Leni, Z., Keller, A., Brem, B.T., Siegerist, F., Schönenberger, D., Durdina, L., Elser, M., Salathe, M., 2022. Responses of reconstituted human bronchial epithelia from normal and health-compromised donors to non-volatile particulate matter emissions from an aircraft turbofan engine. *Environ. Pollut.* 307, 119521.
- Dilger, M., Armant, O., Ramme, L., Mühlhopt, S., Sapcariu, S.C., Schlager, C., Dilger, E., Reda, A., Orasche, J., Schnelle-Kreis, J., 2023. Systems toxicology of complex wood combustion aerosol reveals gaseous carbonyl compounds as critical constituents. *Environ. Int.* 179, 108169.
- Drinovec, L., Močnik, G., Zotter, P., Prévôt, A., Ruckstuhl, C., Coz, E., Rupakheti, M., Sciare, J., Müller, T., Wiedensohler, A., 2015. The "dual-spot" Aethalometer: an improved measurement of aerosol black carbon with real-time loading compensation. *Atmos. Meas. Tech.* 8 (5), 1965–1979.
- EEA, 2021. *Health Impacts of Air Pollution in Europe, 2021*.
- Ehrhardt, C., Forbes, B., Kim, K.-J., 2008. In vitro models of the tracheo-bronchial epithelium. *Drug Absorption Studies: in Situ, in Vitro and in Silico Models*, pp. 235–257.
- Forest, V., 2021. Combined effects of nanoparticles and other environmental contaminants on human health - an issue often overlooked. *NanoImpact* 23, 100344. <https://doi.org/10.1016/j.impact.2021.100344>.
- Gan, M., Ding, H., Chen, G., 2020. 6-Formylindolo[3,2-b]carbazole reduces apoptosis induced by benzo[a]pyrene in a mitochondrial-dependent manner. *Cell Biol. Int.* 44 (12), 2427–2437. <https://doi.org/10.1002/cbin.11450>.
- Gawliotta, N., Orasche, J., Geldenhuys, G.-L., Jakobi, G., Wattrus, M., Jennerwein, M., Michalke, B., Gröger, T., Forbes, P., Zimmermann, R., 2023. A study on the chemical profile and the derived health effects of heavy-duty machinery aerosol with a focus on the impact of alternative fuels. *Air Quality, Atmosphere & Health* 16 (3), 535–551. <https://doi.org/10.1007/s11869-022-01287-9>.
- Ghio, A.J., 1999. Metals associated with both the water-soluble and insoluble fractions of an ambient air pollution particle catalyze an oxidative stress. *Inhal. Toxicol.* 11 (1), 37–49.
- Gualtieri, M., Grollino, M.G., Consales, C., Costabile, F., Manigrasso, M., Avino, P., Aufderheide, M., Cordelli, E., Di Liberto, L., Petralia, E., 2018. Is it the time to study air pollution effects under environmental conditions? A case study to support the shift of in vitro toxicology from the bench to the field. *Chemosphere* 207, 552–564.
- Hamid, R., Rotshteyn, Y., Rabadi, L., Parikh, R., Bullock, P., 2004. Comparison of alamar blue and MTT assays for high through-put screening. *Toxicol. Vitro* 18 (5), 703–710.
- He, R., W., Braakhuis, H.M., Vandebriel, R.J., Staal, Y.C., Gremmer, E.R., Fokkens, P.H., Kemp, C., Vermeulen, J., Westerink, R.H., Cassee, F.R., 2021. Optimization of an air-liquid interface in vitro cell co-culture model to estimate the hazard of aerosol exposures. *J. Aerosol Sci.* 153, 105703.
- Hsiao, W.W., Mo, Z.-Y., Fang, M., Shi, X.-m., Wang, F., 2000. Cytotoxicity of PM_{2.5} and PM_{2.5-10} ambient air pollutants assessed by the MTT and the Comet assays. *Mutation Research/Genetic Toxicology and Environmental Mutagenesis* 471 (1–2), 45–55.
- IARC, 2010. Some non-heterocyclic polycyclic aromatic hydrocarbons and some related exposures. *IARC Monogr. Eval. Carcinog. Risks Hum.* 92, 1.
- Jiang, N., Wen, H., Zhou, M., Lei, T., Shen, J., Zhang, D., Wang, R., Wu, H., Jiang, S., Li, W., 2020. Low-dose combined exposure of carboxylated black carbon and heavy metal lead induced potentiation of oxidative stress, DNA damage, inflammation, and apoptosis in BEAS-2B cells. *Ecotoxicol. Environ. Saf.* 206, 111388. <https://doi.org/10.1016/j.ecoenv.2020.111388>.
- Jonsdottir, H.R., Delaval, M., Leni, Z., Keller, A., Brem, B.T., Siegerist, F., Schönenberger, D., Durdina, L., Elser, M., Burtcher, H., 2019. Non-volatile particle emissions from aircraft turbine engines at ground-idle induce oxidative stress in bronchial cells. *Commun. Biol.* 2 (1), 90.
- Juarez Facio, A.T., Yon, J., Corbiere, C., Rogez-Florent, T., Castilla, C., Lavanant, H., Mignot, M., Devouge-Boyer, C., Logie, C., Chevalier, L., Vaugeois, J.M., Monteil, C., 2022. Toxicological impact of organic ultrafine particles (UFPs) in human bronchial epithelial BEAS-2B cells at air-liquid interface. *Toxicol. Vitro* 78, 105258. <https://doi.org/10.1016/j.tiv.2021.105258>.
- Jung, K.H., Yan, B., Chillrud, S.N., Perera, F.P., Whyatt, R., Camann, D., Kinney, P.L., Miller, R.L., 2010. Assessment of benzo (a) pyrene-equivalent carcinogenicity and mutagenicity of residential indoor versus outdoor polycyclic aromatic hydrocarbons

- exposing young children in New York City. *Int. J. Environ. Res. Publ. Health* 7 (5), 1889–1900.
- Kelly, F.J., Fussell, J.C., 2012. Size, source and chemical composition as determinants of toxicity attributable to ambient particulate matter. *Atmos. Environ.* 60, 504–526. <https://doi.org/10.1016/j.atmosenv.2012.06.039>.
- Kim, S.Y., Kim, S.H., Wee, J.H., Min, C., Han, S.M., Kim, S., Choi, H.G., 2021. Short and long term exposure to air pollution increases the risk of ischemic heart disease. *Sci. Rep.* 11 (1), 5108. <https://doi.org/10.1038/s41598-021-84587-x>.
- Kurtz, M.L., Orona, N.S., Lezón, C., Defosse, V.C., Astort, F., Maglione, G.A., Boyer, P.M., Tasat, D.R., 2024. Decreased immune response in undernourished rats after air pollution exposure. *Environ. Toxicol. Pharmacol.*, 104400.
- Kwon, H.S., Ryu, M.H., Carlsten, C., 2020. Ultrafine particles: unique physicochemical properties relevant to health and disease. *Exp. Mol. Med.* 52 (3), 318–328. <https://doi.org/10.1038/s12276-020-0405-1>.
- Kyung, S.Y., Jeong, S.H., 2020. Particulate-matter related respiratory diseases. *Tuberc. Respir. Dis.* 83 (2), 116–121. <https://doi.org/10.4046/trd.2019.0025>.
- Livak, K.J., Schmittgen, T.D., 2001. Analysis of relative gene expression data using real-time quantitative PCR and the 2(-Delta Delta C(T)) Method. *Methods* 25 (4), 402–408. <https://doi.org/10.1006/meth.2001.1262>.
- Lu, C.F., Li, L.Z., Zhou, W., Zhao, J., Wang, Y.M., Peng, S.Q., 2017. Silica nanoparticles and lead acetate co-exposure triggered synergistic cytotoxicity in A549 cells through potentiation of mitochondria-dependent apoptosis induction. *Environ. Toxicol. Pharmacol.* 52, 114–120. <https://doi.org/10.1016/j.etap.2017.04.001>.
- Lucci, F., Castro, N.D., Rostami, A.A., Oldham, M.J., Hoeng, J., Pithawalla, Y.B., Kuczaj, A.K., 2018. Characterization and modeling of aerosol deposition in Vitrocell® exposure systems-exposure well chamber deposition efficiency. *J. Aerosol Sci.* 123, 141–160.
- Moreno-Ríos, A.L., Tejada-Benítez, L.P., Bustillo-Lecompte, C.F., 2022. Sources, characteristics, toxicity, and control of ultrafine particles: an overview. *Geosci. Front.* 13 (1). <https://doi.org/10.1016/j.gsf.2021.101147>.
- Morgan, T.E., Davis, D.A., Iwata, N., Tanner, J.A., Snyder, D., Ning, Z., Kam, W., Hsu, Y.-T., Winkler, J.W., Chen, J.-C., 2011. Glutamatergic neurons in rodent models respond to nanoscale particulate urban air pollutants in vivo and in vitro. *Environ. Health Perspect.* 119 (7), 1003–1009.
- Müllhopt, S., Dilger, M., Diabaté, S., Schlager, C., Krebs, T., Zimmermann, R., Buters, J., Oeder, S., Wäscher, T., Weiss, C., Paur, H.-R., 2016. Toxicity testing of combustion aerosols at the air-liquid interface with a self-contained and easy-to-use exposure system. *J. Aerosol Sci.* 96, 38–55. <https://doi.org/10.1016/j.jaerosci.2016.02.005>.
- Murray, C.J., Aravkin, A.Y., Zheng, P., Abbafati, C., Abbas, K.M., Abbasi-Kangevari, M., et al., 2020. Global burden of 87 risk factors in 204 countries and territories, 1990–2019: a systematic analysis for the Global Burden of Disease Study 2019. *Lancet* 396 (10258), 1223–1249. [https://doi.org/10.1016/S0140-6736\(20\)30752-2](https://doi.org/10.1016/S0140-6736(20)30752-2).
- Oeder, S., Kanashova, T., Sippula, O., Sapcariu, S.C., Streibel, T., Arteaga-Salas, J.M., Passig, J., Dilger, M., Paur, H.R., Schlager, C., Müllhopt, S., Diabaté, S., Weiss, C., Stengel, B., Rabe, R., Harndorf, H., Torvela, T., Jokiniemi, J.K., Hirvonen, M.R., Zimmermann, R., 2015. Particulate matter from both heavy fuel oil and diesel fuel shipping emissions show strong biological effects on human lung cells at realistic and comparable in vitro exposure conditions. *PLoS One* 10 (6), e0126536. <https://doi.org/10.1371/journal.pone.0126536>.
- Offer, S., Hartner, E., Di Bucchianico, S., Bisig, C., Bauer, S., Pantzke, J., Zimmermann, E. J., Cao, X., Binder, S., Kuhn, E., Huber, A., Jeong, S., Kafer, U., Martens, P., Mescerjakovas, A., Bendl, J., Brejcha, R., Buchholz, A., Gat, D., Zimmermann, R., 2022. Effect of atmospheric aging on soot particle toxicity in lung cell models at the air-liquid interface: differential toxicological impacts of biogenic and anthropogenic secondary organic aerosols (SOAs). *Environ. Health Perspect.* 130 (2), 27003. <https://doi.org/10.1289/EHP9413>.
- Ohlwein, S., Kappeler, R., Kutlar Joss, M., Kunzli, N., Hoffmann, B., 2019. Health effects of ultrafine particles: a systematic literature review update of epidemiological evidence. *Int. J. Publ. Health* 64 (4), 547–559. <https://doi.org/10.1007/s00038-019-01202-7>.
- Ohura, T., Noda, T., Amagai, T., Fusaya, M., 2005. Prediction of personal exposure to PM_{2.5} and carcinogenic polycyclic aromatic hydrocarbons by their concentrations in residential microenvironments. *Environ. Sci. Technol.* 39 (15), 5592–5599.
- Pantzke, J., Koch, A., Zimmermann, E.J., Rastak, N., Offer, S., Bisig, C., Bauer, S., Oeder, S., Orasche, J., Fiala, P., Stintz, M., Ruger, C.P., Streibel, T., Di Bucchianico, S., Zimmermann, R., 2023. Processing of carbon-reinforced construction materials releases PM_{2.5} inducing inflammation and (secondary) genotoxicity in human lung epithelial cells and fibroblasts. *Environ. Toxicol. Pharmacol.* 98, 104079. <https://doi.org/10.1016/j.etap.2023.104079>.
- Petzold, A., Ogren, J.A., Fiebig, M., Laj, P., Li, S.-M., Baltensperger, U., Holzer-Popp, T., Kinne, S., Pappalardo, G., Sugimoto, N., 2013. Recommendations for reporting "black carbon" measurements. *Atmos. Chem. Phys.* 13 (16), 8365–8379.
- Ranzani, O., Alari, A., Olmos, S., Mila, C., Rico, A., Ballester, J., Basagana, X., Chaccour, C., Dadvand, P., Duarte-Salles, T., Foraster, M., Nieuwenhuijsen, M., Sunyer, J., Valentin, A., Kogevinas, M., Lazzano, U., Avellaneda-Gomez, C., Vivanco, R., Tonne, C., 2023. Long-term exposure to air pollution and severe COVID-19 in Catalonia: a population-based cohort study. *Nat. Commun.* 14 (1), 2916. <https://doi.org/10.1038/s41467-023-38469-7>.
- Ravanbakhsh, M., Yousefi, H., Lak, E., Ansari, M.J., Suksatan, W., Qasim, Q.A., Asban, P., Kianizadeh, M., Mohammadi, M.J., 2023. Effect of polycyclic aromatic hydrocarbons (PAHs) on respiratory diseases and the risk factors related to cancer. *Polycycl. Aromat. Comp.* 43 (9), 8371–8387.
- Reinmuth-Selzle, K., Kampf, C.J., Lucas, K., Lang-Yona, N., Frohlich-Nowoisky, J., Shiraiwa, M., Lakey, P.S.J., Lai, S., Liu, F., Kunert, A.T., Ziegler, K., Shen, F., Sgarbanti, R., Weber, B., Bellinghausen, I., Saloga, J., Weller, M.G., Duschl, A., Schuppan, D., Poschl, U., 2017. Air pollution and climate change effects on allergies in the anthropocene: abundance, interaction, and modification of allergens and adjuvants. *Environ. Sci. Technol.* 51 (8), 4119–4141. <https://doi.org/10.1021/acs.est.6b04908>.
- Ren, J., Zhao, G., Sun, X., Liu, H., Jiang, P., Chen, J., Wu, Z., Peng, D., Fang, Y., Zhang, C., 2017. Identification of plasma biomarkers for distinguishing bipolar depression from major depressive disorder by iTRAQ-coupled LC-MS/MS and bioinformatics analysis. *Psychoneuroendocrinology* 86, 17–24.
- Rothen-Rutishauser, B., Gibb, M., He, R., Petri-Fink, A., Sayes, C.M., 2023. Human lung cell models to study aerosol delivery - considerations for model design and development. *Eur. J. Pharmaceut. Sci.* 180, 106337. <https://doi.org/10.1016/j.ejps.2022.106337>.
- Rstudio, T., 2020. RStudio: Integrated Development for R. *Rstudio Team*. PBC, Boston, MA. URL.
- Shimada, T., Inoue, K., Suzuki, Y., Kawai, T., Azuma, E., Nakajima, T., Shindo, M., Kurose, K., Sugie, A., Yamagishi, Y., Fujii-Kuriyama, Y., Hashimoto, M., 2002. Arylhydrocarbon receptor-dependent induction of liver and lung cytochromes P450 1A1, 1A2, and 1B1 by polycyclic aromatic hydrocarbons and polychlorinated biphenyls in genetically engineered C57BL/6J mice. *Carcinogenesis* 23 (7), 1199–1207. <https://doi.org/10.1093/carcin/23.7.1199>.
- Stafoggia, M., Oftedal, B., Chen, J., Rodopoulou, S., Renzi, M., Atkinson, R.W., Bauwelinck, M., Klompaker, J.O., Mehta, A., Vienneau, D., 2022. Long-term exposure to low ambient air pollution concentrations and mortality among 28 million people: results from seven large European cohorts within the ELAPSE project. *Lancet Planet. Health* 6 (1), e9–e18.
- Stewart, C.E., Torr, E.E., Mohd Jamili, N.H., Bosquillon, C., Sayers, I., 2012. Evaluation of differentiated human bronchial epithelial cell culture systems for asthma research. *J. Allergy* 2012 (1), 943982.
- Strak, M., Hoek, G., Steenhouf, M., Kilinc, E., Godri, K.J., Gosens, I., Mudway, I.S., van Oerle, R., Spronk, H.M., Cassee, F.R., 2013. Components of ambient air pollution affect thrombin generation in healthy humans: the RAPTES project. *Occup. Environ. Med.* 70 (5), 332–340.
- Strak, M., Weinmayr, G., Rodopoulou, S., Chen, J., De Hoogh, K., Andersen, Z.J., Atkinson, R., Bauwelinck, M., Bekkevold, T., Bellander, T., 2021. Long term exposure to low level air pollution and mortality in eight European cohorts within the ELAPSE project: pooled analysis. *BMJ* 374.
- Team, R.C., 2020. R: A Language and Environment for Statistical Computing. R Foundation for Statistical Computing.
- Thurston, G.D., Rice, M.B., 2019. Air pollution exposure and asthma incidence in children: demonstrating the value of air quality standards. *JAMA* 321 (19), 1875–1877. <https://doi.org/10.1001/jama.2019.5343>.
- Tsai, D.H., Riediker, M., Berchet, A., Paccaud, F., Waeber, G., Vollenweider, P., Bochud, M., 2019. Effects of short- and long-term exposures to particulate matter on inflammatory marker levels in the general population. *Environ. Sci. Pollut. Res. Int.* 26 (19), 19697–19704. <https://doi.org/10.1007/s11356-019-05194-y>.
- Upadhyay, S., Palmberg, L., 2018. Air-liquid interface: relevant in vitro models for investigating air pollutant-induced pulmonary toxicity. *Toxicol. Sci.* 164 (1), 21–30. <https://doi.org/10.1093/toxsci/kfy053>.
- Weber, S.A., Insaif, T.Z., Hall, E.S., Talbot, T.O., Huff, A.K., 2016. Assessing the impact of fine particulate matter (PM_{2.5}) on respiratory-cardiovascular chronic diseases in the New York City Metropolitan area using Hierarchical Bayesian Model estimates. *Environ. Res.* 151, 399–409.
- Wei, S., Liao, J., Xue, T., Yu, K., Fu, X., Wang, R., Dang, X., Zhang, C., Qiao, H., Jiang, S., Xiao, J., Dong, L., Yin, J., Yan, X., Jia, W., Zhang, G., Chen, R., Zhou, B., Song, B., Wang, G., 2023. Ambient fine particulate matter and allergic symptoms in the middle-aged and elderly population: results from the PIFCOPD study. *Respir. Res.* 24 (1), 139. <https://doi.org/10.1186/s12931-023-02433-2>.
- Weichenthal, S., Pinault, L., Christidis, T., Burnett, R.T., Brook, J.R., Chu, Y., Crouse, D. L., Erickson, A.C., Hystad, P., Li, C., 2022. How low can you go? Air pollution affects mortality at very low levels. *Sci. Adv.* 8 (39), eabo3381.
- WHO, 2021a. New WHO Global Air Quality Guidelines Aim to Save Millions of Lives from Air Pollution.
- WHO, 2021b. WHO Global Air Quality Guidelines: Particulate Matter (PM_{2.5} and PM₁₀), Ozone, Nitrogen Dioxide, Sulfur Dioxide and Carbon Monoxide: Executive Summary.
- Yu, Y.-y., Jin, H., Lu, Q., 2022. Effect of polycyclic aromatic hydrocarbons on immunity. *Journal of Translational Autoimmunity* 5, 100177.
- Zavala, J., Greenan, R., Krantz, Q.T., DeMarini, D.M., Higuchi, M., Gilmour, M.I., White, P.A., 2017. Regulating temperature and relative humidity in air-liquid interface in vitro systems eliminates cytotoxicity resulting from control air exposures. *Toxicol. Res.* 6 (4), 448–459. <https://doi.org/10.1039/c7tx00109f>.
- Zheng, D., Wang, N., Wang, X., Tang, Y., Zhu, L., Huang, Z., Tang, H., Shi, Y., Wu, Y., Zhang, M., Lu, B., 2012. Effects of the interaction of TiO₂ nanoparticles with bisphenol A on their physicochemical properties and in vitro toxicity. *J. Hazard Mater.* 199–200, 426–432. <https://doi.org/10.1016/j.jhazmat.2011.11.040>.
- Zimmermann, E.J., Candeias, J., Gawlitta, N., Bisig, C., Binder, S., Pantzke, J., Offer, S., Rastak, N., Bauer, S., Huber, A., Kuhn, E., Buters, J., Groeger, T., Delaval, M.N., Oeder, S., Di Bucchianico, S., Zimmermann, R., 2023. Biological impact of sequential exposures to allergens and ultrafine particle-rich combustion aerosol on human bronchial epithelial BEAS-2B cells at the air liquid interface. *J. Appl. Toxicol.* <https://doi.org/10.1002/jat.4458>.
- Zotter, P., Herich, H., Gysel, M., El-Haddad, I., Zhang, Y., Močnik, G., Hüglin, C., Baltensperger, U., Szidat, S., Prévôt, A.S., 2017. Evaluation of the absorption Ångström exponents for traffic and wood burning in the Aethalometer-based source apportionment using radiocarbon measurements of ambient aerosol. *Atmos. Chem. Phys.* 17 (6), 4229–4249.